Optimising finite-time photon extraction from emitter-cavity systems: supplemental document

1. CALCULATING PROBABILITY FUNCTIONS FOR ANALYTIC METHOD

The probabilities used in Sec. 2.2 of the main text can be expressed in terms of the integral notation of Eq. (6), restated below for clarity

$$I_{(nm)}(t) = \int_0^t \left(\overset{n\cdot}{\alpha_g} \overset{m\cdot *}{\alpha_g} + \overset{m\cdot}{\alpha_g} \overset{n\cdot *}{\alpha_g} \right) dt, \tag{S1}$$

where $n\cdot$ is a shorthand for n copies of $\cdot$ indicating n time derivatives.

Firstly, the probability P_κ that there has been decay from the cavity mode is given by

$$\begin{aligned} P_\kappa(t) &= 2\kappa \int_0^t \left|\alpha_g(t')\right|^2 dt', \\ &= \kappa \int_0^t \alpha_g(t')\alpha_g^*(t') + \alpha_g^*(t')\alpha_g(t')\, dt', \\ &= \kappa I_{(00)}(t), \end{aligned} \tag{S2}$$

where the final line follows from the definition of the notation in Eq. (S1).

The probability that the state is $|g,1\rangle$ can be written similarly through

$$\begin{aligned} P_g(t) &= \left|\alpha_g(t)\right|^2, \\ &= \int_0^t \frac{d}{dt'} \left(\left|\alpha_g(t')\right|^2 \right) dt', \\ &= \int_0^t \alpha_g(t')\dot{\alpha_g}^*(t') + \dot{\alpha_g}(t')\alpha_g^*(t') dt', \\ &= I_{(10)}(t), \end{aligned} \tag{S3}$$

where the second line follows from the first because the state $|g,1\rangle$ is unoccupied at the start of the process.

The probability $P_\gamma(t)$ of spontaneous emission before time t and $P_e(t)$ of occupation of state $|e,0\rangle$ at time t are derived in a similar fashion, using Eq. (5) from the main text, which is restated below:

$$\alpha_e = -\frac{1}{g}\left(\kappa\alpha_g + \dot{\alpha_g}\right). \tag{S4}$$

This relation may be substituted into the integral form for the spontaneous emission probability,

$$P_\gamma(t) = 2\gamma \int_0^t \left|\alpha_e(t')\right|^2 dt', \tag{S5}$$

to yield

$$P_\gamma(t) = \frac{\gamma\kappa^2}{g^2} I_{(00)}(t) + \frac{2\gamma\kappa}{g^2} I_{(10)}(t) + \frac{\gamma}{g^2} I_{(11)}(t). \tag{S6}$$

Finally, the probability $P_e(t)$ that state $|e,0\rangle$ is occupied at time t can be derived

$$\begin{aligned} P_e(t) &= |\alpha_e(t)|^2, \\ &= \int_0^t \frac{d}{dt'} \left(\left|\alpha_e(t')\right|^2 \right) dt', + |\alpha_e(0)|^2 \\ &= \int_0^t \left| -\frac{1}{g}\left(\kappa\alpha_g(t') + \dot{\alpha_g}(t')\right) \right|^2 + \left| -\frac{1}{g}\left(\kappa\alpha_g(0) + \dot{\alpha_g}(0)\right) \right|^2 \\ &= \frac{\kappa^2}{g^2} I_{(10)}(t) + \frac{\kappa}{g^2} I_{(20)}(t) + \frac{\kappa}{g^2} I_{(11)}(t) + \frac{1}{g^2} I_{(21)}(t) + \frac{1}{g^2} |\dot{\alpha_g}(0)|^2, \end{aligned} \tag{S7}$$

where the third line follows from the second through the substitution of Eq. (S4), and the fourth from the third through the integral definitions Eq. (S1) and the initial condition $\alpha_g(0) = 0$.

The results of this appendix are summarised

$$\begin{aligned}
P_\kappa(t) &= \kappa I_{(00)}(t), \\
P_g(t) &= I_{(10)}(t), \\
P_\gamma(t) &= \frac{\gamma\kappa^2}{g^2} I_{(00)}(t) + \frac{2\gamma\kappa}{g^2} I_{(10)}(t) + \frac{\gamma}{g^2} I_{(11)}(t), \\
P_e(t) &= \frac{\kappa^2}{g^2} I_{(10)}(t) + \frac{\kappa}{g^2} I_{(20)}(t) + \frac{\kappa}{g^2} I_{(11)}(t) + \frac{1}{g^2} I_{(21)}(t) + \frac{1}{g^2}\left|\dot{\alpha_g}(0)\right|^2, \\
P_u(t) &= 1 - P_\kappa(t) + P_g(t) + P_\gamma(t) + P_e(t).
\end{aligned} \tag{S8}$$

2. THE ANALYTIC UPPER BOUND DOES NOT HAVE A HYPERBOLIC SOLUTION

The wavefunction amplitude α_g of the occupied cavity state for the upper bound of the emission probability satisfies Eq. (14) of the main text, which is written below for clarity

$$\ddot{\alpha_g} + \kappa^2 (2Cq - 1)\, \alpha_g = 0, \tag{S9}$$

where κ is the cavity amplitude decay rate, C is the cooperativity, and q is a positive scalar. On the assumption that $2Cq - 1 < 0$, the solutions to Eq. (S9) for $\alpha_g(t)$ are hyperbolic. The boundary condition that $\alpha_g(0) = 0$ means that the form must be a hyperbolic sine. Specifically, α_g satisfies

$$\begin{aligned}
\alpha_g &= A \sinh(st), \\
s &= \sqrt{\kappa^2 (1 - 2Cq)},
\end{aligned} \tag{S10}$$

where A is an undetermined amplitude. Substituting this wavefunction form into the equation for the system probabilities (Eq. (7) from the main text) leads to

$$\begin{aligned}
P_\kappa(t) &= A^2\kappa \left(\frac{1}{2s} \sinh(2st) - t \right), \\
P_g(t) &= A^2 \sinh^2(st), \\
P_\gamma(t) &= A^2 \left\{ \frac{\gamma\kappa^2}{g^2} \left(\frac{1}{2s} \sinh(2st) - t \right) + \frac{2\gamma\kappa}{g^2} \sinh^2(st) + \frac{\gamma s^2}{g^2} \left(\frac{1}{2s} \sinh(2st) + t \right) \right\}.
\end{aligned} \tag{S11}$$

The second condition satisfied by the upper bound is that $q = m$ where $m = (P_g(T) + P_\gamma(T))/P_\kappa(T)$ (Eq. (9) from the main text). Evaluating m with the probabilities from Eq. (S11) gives

$$m = \frac{1}{2C} + \frac{\left(\frac{2\gamma}{g^2} + 1\right) \sinh^2(sT) + \frac{\gamma s^2}{\kappa g^2} \left(\frac{1}{2s} \sinh(2sT) + T \right)}{\frac{1}{2s} \sinh(2sT) - T}. \tag{S12}$$

The positivity of each term of the right hand side quotient for $T > 0$ implies that $m \geq 1/2C$. This means that q cannot equal m and be consistent with our assumption that $2Cq - 1 < 0$. Therefore the hyperbolic case is never a solution for the upper bound wavepacket.

3. CALCULATING PROBABILITY MATRICES FOR THE NUMERIC METHOD

All probabilities $P_\zeta(t)$ used in the optimisation can be expressed as expectation values of matrices $\hat{P_\zeta}(t)$ for Fourier vector $\overrightarrow{\alpha_{g_1}^F}$. The simplest example is $P_{\kappa_1}(t)$:

$$
\begin{aligned}
P_{\kappa_1}(t) &= 2\kappa \int_0^t \alpha^*_{g_1}(t')\alpha_{g_1}(t')\,dt', \\
&= \frac{2\kappa}{T_b}\int_0^t \sum_{n,n'} C^{(1)*}_{n'} C^{(1)}_n e^{i(\omega_n-\omega_{n'})t'}\,dt', \\
&= \sum_{n,n'} C^{(1*)}_{n'}(2\kappa \hat{V}_{n',n}(t))C^{(1)}_n, \\
&= \overrightarrow{\alpha^F_{g_1}}^{\dagger}\cdot 2\kappa\hat{V}\cdot\overrightarrow{\alpha^F_{g_1}}, \\
\hat{V}_{n',n}(t) &= \frac{1}{T_b}\int_0^t e^{i(\omega_n-\omega_{n'})t'}\,dt'.
\end{aligned}
\tag{S13}
$$

This can be generalised to other emission probabilities by using the interdependence of the wavefunctions through

$$
\begin{aligned}
P_{\kappa_j} &= \sum_{n,n'} C^{(j)*}_{n'}(2\kappa\hat{V}_{n',n})C^{(j)}_n, \\
&= \overrightarrow{\alpha^F_{g_1}}^{\dagger}\cdot\left(2\kappa\hat{F}^{(j)\dagger}\hat{V}(t)\hat{F}^{(j)}\right)\cdot\overrightarrow{\alpha^F_{g_1}}, \\
\hat{F}^{(j)}_{n',n} &= f^{(1\to j)}_n\delta_{n',n},
\end{aligned}
\tag{S14}
$$

where δ is the Kronecker delta, leading to the component form

$$
\hat{P_{\kappa_j}}_{n',n}(t) = 2\kappa(f^{(1\to j)}_{n'})^*\hat{V}_{n',n}(t)f^{(1\to j)}_n. \tag{S15}
$$

For the cavity probabilities, the probability

$$
\begin{aligned}
P_{g_j}(t) &= |\alpha_{g_j}(t)|^2, \\
&= \sum_{n,n'} C^{(1)*}_{n'}\left[(f^{(1\to j)}_n)^*(\exp\{i(\omega_n-\omega_{n'})t\})f^{(1\to j)}_n\right]C^{(1)}_n, \\
&= \overrightarrow{\alpha^F_{g_1}}^{\dagger}\cdot\hat{P_{g_j}}\cdot\overrightarrow{\alpha^F_{g_1}}, \\
\hat{P_{g_j}}_{n',n}(t) &= (f^{(1\to j)}_{n'})^*(\exp\{i(\omega_n-\omega_{n'})t\})f^{(1\to j)}_n,
\end{aligned}
\tag{S16}
$$

is most easily expressed through a matrix given in component form.

The calculation for the spontaneous emission probability requires the expression for the excited state component (taken from Eq. (19) of the main text)

$$
\alpha_e(t) = -\frac{\kappa+i\Delta_{g_1}}{g_1}\alpha_{g_1} - \frac{1}{g_1}\dot{\alpha_{g_1}}. \tag{S17}
$$

From this, the spontaneous emission probability

$$
\begin{aligned}
P_\gamma(t) &= 2\gamma\int_0^t \alpha^*_e(t')\alpha_e(t')\,dt', \\
&= \overrightarrow{\alpha^F_{g_1}}^{\dagger}\cdot\hat{P_\gamma}(t)\cdot\overrightarrow{\alpha^F_{g_1}}, \\
\hat{P_\gamma}_{n',n}(t) &= \frac{2\gamma}{g_1^2}\left[\kappa^2+\Delta^2_{g_1}+i\kappa(\omega_n-\omega_{n'})+\Delta_{g_1}(\omega_n+\omega_{n'})+\omega_n\omega_{n'}\right]\hat{V}_{n',n}(t),
\end{aligned}
\tag{S18}
$$

can be expressed. The matrix for probability $P_e(t) = |\alpha_e(t)|^2$ in the excited state at time t can also be written in a similar component form

$$
\hat{P}_{en',n}(t) = \frac{1}{g_1^2 T_b}\left[\kappa^2+\Delta^2_{g_1}+i\kappa\left(\omega_n-\omega_{n'}\right)+\Delta_{g_1}\left(\omega_n+\omega_{n'}\right)+\omega_n\omega_{n'}\right]\exp\left\{i(\omega_n-\omega_{n'})t\right\}. \tag{S19}
$$

In order to calculate results numerically, the $\hat{V}_{n',n}(t)$ can be evaluated exactly

$$
\hat{V}_{n',n}(t) = \begin{array}{ll} \dfrac{2}{T_b\left(\omega_n-\omega_{n'}\right)}\sin\left(\dfrac{1}{2}\left(\omega_n-\omega_{n'}\right)t\right)\exp\left(\dfrac{1}{2}i\left(\omega_n-\omega_{n'}\right)t\right), & \omega_n\neq\omega_{n'}, \\ \dfrac{t}{T_b}, & \omega_n=\omega_{n'}. \end{array} \tag{S20}
$$

The matrices derived in this section can be summarised in component notation:

$$\begin{aligned}
\hat{P_{\kappa_j}}_{n',n}(t) &= 2\kappa(f_{n'}^{(1\to j)})^*\hat{V}_{n',n}(t)f_n^{(1\to j)},\\
\hat{P_{g_j}}_{n',n}(t) &= (f_{n'}^{(1\to j)})^*(\exp\{i(\omega_n-\omega_{n'})t\})f_n^{(1\to j)},\\
\hat{P_{\gamma}}_{n',n}(t) &= \frac{2\gamma}{g_1^2}\left[\kappa^2+\Delta_{g_1}^2+i\kappa(\omega_n-\omega_{n'})+\Delta_{g_1}(\omega_n+\omega_{n'})+\omega_n\omega_{n'}\right]\hat{V}_{n',n}(t),\\
\hat{P}_{en',n}(t) &= \frac{1}{g_1^2T_b}\left[\kappa^2+\Delta_{g_1}^2+i\kappa\left(\omega_n-\omega_{n'}\right)+\Delta_{g_1}\left(\omega_n+\omega_{n'}\right)+\omega_n\omega_{n'}\right]\exp\left\{i(\omega_n-\omega_{n'})t\right\}.
\end{aligned} \tag{S21}$$

4. CALCULATING THE REQUIRED DRIVING PULSE

Given a photon wavepacket $\alpha_{g_1}(t)$ for the numeric method (or equivalently $\alpha_g(t)$ for the analytic method), the driving to produce this wavepacket can be calculated. In practice, the driving should be calculated for $\alpha_{g_1}(t)=(1-\chi)\alpha_{g_1}^S(t)$, where $\alpha_{g_1}^S(t)$ is the ideal solution and χ is a small number. This is because the ideal solution is on the bounds of physical possibility, and therefore the driving required to produce it will tend to infinite strength at the end of the process [1]. Reducing the overall amplitude slightly removes this tendency. This is in analogy with an aspect of photon absorption where a photon wavepacket cannot be absorbed optimally by an emitter-cavity system without a singularity in the control drive at the initial time [2].

Taking the equations of motion (Eq. (19) from the main text), all variables except the complex driving amplitude Ω and the obtained cavity output functions $\left\{\alpha_{g_j}(t)\right\}$ can be eliminated to produce a differential equation

$$\begin{aligned}
\dot{\Omega}\left[\tilde{\kappa}\tilde{\gamma}\alpha_{g_1}+(\tilde{\kappa}+\tilde{\gamma})\dot{\alpha_{g_1}}+\ddot{\alpha_{g_1}}+g_1\sum_{j=1}^{j_M}(g_j\alpha_{g_j})\right] &= \\
\Omega[i\Delta_u\tilde{\kappa}\tilde{\gamma}\alpha_{g_1}+(\tilde{\kappa}\tilde{\gamma}+i\Delta_u(\tilde{\kappa}+\tilde{\gamma}))\dot{\alpha_{g_1}}& \\
+(\tilde{\kappa}+\tilde{\gamma}+i\Delta_u)\ddot{\alpha_{g_1}}+\dddot{\alpha_{g_1}}+g_1\sum_{j=1}^{j_M}g_j(i\Delta_u\alpha_{g_j}+\dot{\alpha_{g_j}})]& \\
+|\Omega|^2\Omega(\tilde{\kappa}\alpha_{g_1}+\dot{\alpha_{g_1}})&
\end{aligned} \tag{S22}$$

where $\tilde{\gamma}\equiv\gamma+i\Delta_e$ and $\tilde{\kappa}\equiv\kappa+i\Delta_{g_1}$. These equations should be integrated from the initial driving amplitude

$$\begin{aligned}
\Omega^{(\theta_0)}(0,\theta_0) &= -\frac{(\tilde{\kappa}+\tilde{\gamma})\dot{\alpha_{g1}}(0)+\ddot{\alpha_{g1}}(0)}{g_1\alpha_u^{(\theta_0)}(0)},\\
\alpha_u^{(\theta_0)}(0) &= \sqrt{1-|\alpha_e(0)|^2}e^{i\theta_0},\\
\alpha_e(0) &= -\frac{1}{g_1}\dot{\alpha_{g_1}}(0),
\end{aligned} \tag{S23}$$

where the superscript θ_0 indicates that there is freedom in the initial condition. The shape of the cavity output may dictate that there is population in $|e,0\rangle$ at time $t=0$, meaning the initial state is a superposition of $|u,0\rangle$ and $|e,0\rangle$. The phase of this superposition is θ_0, and does not affect whether the photon can be produced, but does affect the drive Ω that produces it.

As discussed in Sec. 2.2 of the main text, it is still possible to achieve the performance predicted from a system initialised to $|u,0\rangle$, but the driving now consists of two parts. The first is an instantaneous (or in practice very fast) excitation that sets up the initial state of Eq. (S23), and the second is specified by Eq. (S22). The relative phase of the two parts of the drive determines θ_0, so must be precisely controlled.

It is important to note, however, that the conditions imposed have not restricted the driving in any way. As such, the drive may contain spikes of intensity where very fast changes in excited state amplitude are required to produce the optimum photon. These spikes can persist even when the target amplitude is reduced from the theoretical maximum amplitude.

The driving pulse derivative equation (Eq. S22) is very sensitive to any numerical artefacts in the cavity output functions $\left\{\alpha_{g_j}(t)\right\}$. This means that the numerically optimised outputs from

the main text can produce driving pulses that have very large swings in amplitude required to produce these artefacts. It is possible to reduce such issues by removing high frequency components from the optimised photon vector $\overrightarrow{\alpha^F_{g_1}}$, but at the cost of distorting the wavepacket.

Once the full quantum dynamics have been calculated, the driving wavepacket can be verified by checking that it is consistent with a rearranged version of Eq. (19) from the main text

$$\Omega = \left(\frac{1}{\alpha_u}\right)\left(\dot{\alpha_e} + \tilde{\gamma}\alpha_e - \sum_{j=1}^{j_M} g_j \alpha_{g_j}\right). \tag{S24}$$

This equation could also be used to predict the driving in the Λ-system case with $\Delta_e = \Delta_u = \theta_0 = 0$. In that situation, the equations of motion (Eq. (4) in the main text) are completely real, so wavefunction component amplitudes α_u, α_e, and α_g can be calculated directly from probabilities with the appropriate choice of sign. This special method for calculating the driving for particular Λ-systems is less sensitive to numerical artefacts than Eq. (S22), but the impact of artefacts is still significant for our data. Therefore, to meaningfully calculate the driving for wavepackets optimised by the numeric procedure would likely require very smooth wavepackets that have been optimised extensively to remove any defects and very high time resolution.

To give a sense of the pulses required, it is possible to calculate the pulses using the lower bound wavepacket. This wavepacket has an analytically defined shape, and there are therefore no numerical artefacts. Examples of the driving required to produce the lower bounds for the case studies of Fig. 3 in the main text were calculated using Eq. S22 and are shown in Fig. S1. This shows how the driving strength required diverges as the probability limits are approached, and that the driving profile required varies considerably with system parameters. Finally, we see that the zeroes of the drive are a feature of the wavepacket shape and not its amplitude (as can be seen simply from Eq. S24).

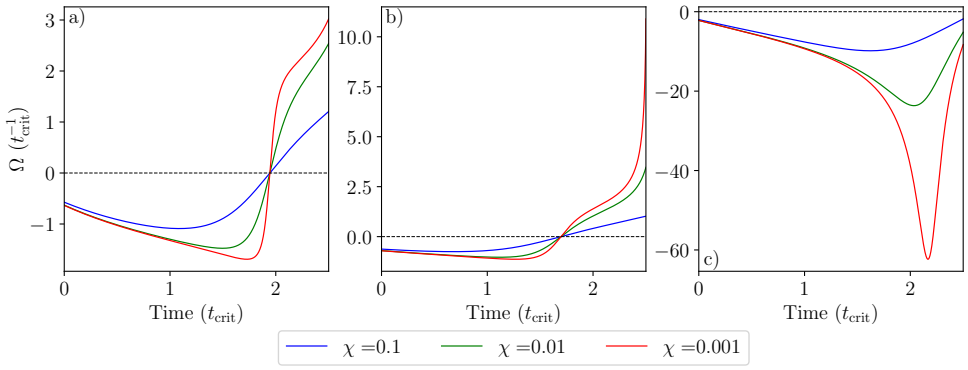

Fig. S1. Driving amplitude required to produce the lower bound wavepacket for the case studies presented in Fig. 3 in the main text, in each case with $\Delta_e = \Delta_u = \theta_0 = 0$. Due to this choice, the driving amplitude Ω is always real in this figure, although for general parameters values Ω is a complex function of time. The plots a), b), and c) correspond to rows a), b), and c) in columns ii) and iii) of Fig. 3 of the main text respectively. The driven photon wavepacket is scaled in amplitude by a factor $(1-\chi)$ compared to the true lower bound, meaning that $\lim_{\chi\to 0}$ produces the lower bound solution and is therefore on the edge of physical possibility.

5. SELECTING NUMERICAL PARAMETERS FOR SIMULATIONS

A. Number of Fourier basis states

The numerical simulations optimise a desired probability by adjusting the vector $\overrightarrow{\alpha^F_{g_1}}$ of amplitudes in a Fourier expansion of $\alpha_{g_1}(t)$. The number of Fourier coefficients used must be sufficient for the situation or the reported optimum will deviate from the true optimum. While there is no precise rule for the number of states that must be used, there are general principles to guide this choice. These can be formulated as conditions on the maximum basis frequency $\omega_{\rm max}$.

Firstly, the basis must be suitable large to describe the photon's temporal profile. This requires

$$\omega_{\max} \gg \frac{2\pi}{\tau}, \tag{S25}$$

where τ is the timescale of the photon. This timescale is at most T (the total emission time of the photon), but for wavepackets with fast rises like the exponential decay solutions (Such as Fig. 3aiii), τ may be considerably shorter than T and the requisite basis size correspondingly bigger.

Secondly, the wavepacket profile $\alpha_{g_1}(t)$ does not necessarily have to go to zero at time T, but, due to the initial condition at $t = 0$ and the periodic temporal behaviour imposed by the Fourier series, must go to zero at the basis time T_b. This means that the basis must be sufficiently large to model the amplitude as it goes to zero between times T and T_b, even if the amplitude in this time window is not physical. This imposes the condition

$$\omega_{\max} \gg \frac{2\pi}{T_b - T}. \tag{S26}$$

Thirdly, with emitter-occupied cavity states detuned from the nominal zero frequency by Δ_{g_j}, the Fourier expansion is likely to contain components at these frequencies. If the largest magnitude detuning in $\left\{\Delta_{g_j}\right\}$ is $\Delta_{\max}$, this imposes the condition

$$\omega_{\max} > \Delta_{\max}. \tag{S27}$$

Finally, to ensure that all emitter-occupied cavity states are initially unoccupied, a total of j_M^d constraints are applied to the solution, where j_M^d is the number of non-degenerate emitter-occupied cavity states (see Sec. 3.3 in the main text). This means that the basis size must be reduced by j_M^d, and therefore must be bigger than j_M^d to begin.

In practice the number of frequency states used for the investigation was typically around 50-100 positive frequencies (with an equal number of negative frequencies and a zero frequency component). However, this number varied significantly depending on the system parameters, with the wavepackets featuring prominent exponential decays generally requiring more components. An important limitation is imposed by the detuning condition Eq. S27 which means that a large number of basis states is required to model systems with large emitter-occupied cavity state energy splittings and long photon production times.

B. Number of normalisation times

The method of ensuring that the probabilities during photon production do not violate probability conservation is described in Sec. 3.4 of the main text. This requires the time $t_{\max}$ at which the probability not contained in the initial state is maximised. To calculate this time, the unnormalised total probability matrix $\hat{P}^P_{\vec{u}}(t)$ was calculated at a discrete series of times throughout the photon production process. At each step during the optimisation process of Eq. (34) in the main text, the maximum time $t_{\max}$ is calculated by finding the total probability matrix with the largest expectation.

A consequence of this method is that, if too few discrete times are chosen for evaluating the total probability, it is possible to violate probability conservation between discrete times, provided probability conservation is satisfied at discrete times. This is likely to be the reason behind the high frequency noise seen in some figures (such as 3bii) or 4d) in the main text), which becomes stronger and lower frequency if the number of discrete times is reduced. The disadvantge to using a large number of discrete times is that the optimisation process takes considerably longer.

6. LIMITING CASES FOR THE REMOTE ENTANGLEMENT CASE STUDY

For the remote entanglement case study (Sec. 4.3 of the main text) we maximise the probability product $P_{\kappa_1} P_{\kappa_2}$ obtained in finite time from a generalised Λ-system with two emitter-occupied cavity states. The cavity coupling of one emitter-occupied cavity state is g_1, and the other g_2, where the corresponding occupied cavity modes, $|1_1\rangle$ and $|1_2\rangle$, are orthogonally-polarised. The energy splitting Δ_Z between the two emitter-occupied cavity states ($|g_1, 1_1\rangle$ and $|g_2, 1_2\rangle$) and the time of photon production T are varied. Simple models can be used to predict the infinite time outputs in the cases that $\Delta_Z = 0$ and $\Delta_Z \to \infty$.

Firstly, in the case of $\Delta_Z = 0$, the excited state actually couples directly to a single level

$$|g_{\text{eff}}, 1_{\text{eff}}\rangle = \frac{g_1 |g_1, 1_1\rangle + g_2 |g_2, 1_2\rangle}{\sqrt{g_1^2 + g_2^2}}, \tag{S28}$$

with an effective coupling $g_{\text{eff}} = \sqrt{g_1^2 + g_2^2}$. This means that the adiabatic limit to the photon emission probability is

$$\begin{aligned} P_{\kappa_{\text{eff}}}^{(a,\Delta_0)} &= \frac{2C_{\text{eff}}}{2C_{\text{eff}} + 1}, \\ C_{\text{eff}} &= \frac{g_{\text{eff}}^2}{2\kappa\gamma}. \end{aligned} \tag{S29}$$

The ratio of this emitted probability labelled P_{κ_1} to the probability labelled P_{κ_2} is $g_1^2 : g_2^2$. The reported success probability in infinite time is therefore

$$P_{\kappa_1\kappa_2}^{(a,\Delta_0)} = \frac{g_1^2 g_2^2}{g_{\text{eff}}^4} \left(P_{\kappa_{\text{eff}}}^{(a,\Delta_0)}\right)^2, \tag{S30}$$

which may be rearranged to

$$P_{\kappa_1\kappa_2}^{(a,\Delta_0)} = \frac{g_1^2 g_2^2}{g_{\text{eff}}^4} \left(\frac{g_{\text{eff}}^2}{g_{\text{eff}}^2 + \kappa\gamma}\right)^2. \tag{S31}$$

Secondly, in the case that Δ_Z becomes large, the production processes for the two components are spectrally decoupled. The decay indexed by $j = \{1, 2\}$ then has a separate cooperativity $C_j = g_j^2/2\kappa\gamma$ and therefore an infinite-time ratio of cavity emission to spontaneous emission of $2C_j : 1$. Note that this argument attributes some of the spontaneous emission probability P_γ to emitter-occupied cavity state 1 and some to emitter-occupied cavity state 2. Though there is no experimental distinction between the spontaneous decay attributed to the two indices, this labelling functions to account for probabilities. If the total probability of either spontaneous emission attributed to decay channel 1 or emitted through emitter-occupied cavity state 1 is f_1, the emitted probability through emitter-occupied cavity state 1 is

$$P_{\kappa_1} = f_1 \frac{2C_1}{2C_1 + 1}, \tag{S32}$$

and equivalently for emitter-occupied cavity state 2 the cavity emission probability is

$$P_{\kappa_2} = f_2 \frac{2C_2}{2C_2 + 1}, \tag{S33}$$

where f_2 is the sum of cavity emission and spontaneous emission attributed to emitter-occupied cavity state 2. As there is no final occupation of the excited state or the emitter-occupied cavity states in the adiabatic regime, for an optimised output the sum of cavity and spontaneous emission outputs should be unity. This means that $f_1 + f_2 = 1$. It is simple to see that the optimum values of f_1 and f_2 are both $1/2$. This leads to an optimised success probability

$$P_{\kappa_1\kappa_2}^{(a,\Delta_\infty)} = \frac{2C_1 2C_2}{4(2C_1 + 1)(2C_2 + 1)}. \tag{S34}$$

REFERENCES

1. G. S. Vasilev, D. Ljunggren, and A. Kuhn, "Single photons made-to-measure," New J. Phys. **12**, 063024 (2010).
2. J. Dilley, P. Nisbet-Jones, B. W. Shore, and A. Kuhn, "Single-photon absorption in coupled atom-cavity systems," Phys. Rev. A **85**, 023834 (2012).